SUPPORTING INFORMATION

Thin free-standing liquid films manipulation: device design to turn on/off gravity in flow regimes for thickness map control and for material structuring

Paolo Iaccarino[a,b,c,‡], Zhe Wang[b,d,‡], Andrea Marfuggi[b,c], Simone Russo[b], Vincenzo Ferraro[b,e], Giuseppe Vitiello[b,f], Sara Coppola[d], and Ernesto Di Maio[b,c,*]

[a]*Scuola Superiore Meridionale, Largo San Marcellino 10, 80125, Naples, Italy*
[b]*Dipartimento di Ingegneria Chimica, dei Materiali e della Produzione Industriale, P.le Tecchio 80, 80125, Naples, Italy*
[c]*foamlab, University of Naples Federico II, P.le Tecchio 80, 80125 Naples, Italy*
[d]*Institute of Applied Sciences and Intelligent Systems "E. Caianiello", Italian National Research Council (ISASI-CNR), Via Campi Flegrei 34, 80078, Pozzuoli (Naples), Italy*
[e]*Dipartimento di Ingegneria e Architettura, University of Parma, Via delle Scienze 181, 43124, Parma, Italy*
[f]*CSGI, Center for Colloid and Surface Science, via della Lastruccia 3, 50019, Florence, Italy*
[*]corresponding author. E-mail: edimaio@unina.it
[‡]These authors contributed equally to this work

1 Viscosity of 10% w/w PVA/water solution

Viscosity of 10% w/w PVA/water solution is measured by using a rheometer (Discovery Hybrid Rheometer 2, TA Instruments, USA), and the result (of two tests) is shown in Figure SI 1. It can be seen that the viscosity (η) is ~ 0.11 Pa·s in the investigated shear rate range.

2 Transmission Electron Microscopy (TEM) analysis of ZnO-NPs

The TEM analysis is used to reveal the morphology of synthesized nanoparticles. The TEM analysis reveals that the synthesized ZnO-NPs possess the desired rod-like morphology, with an average main length of about 30 nm (Figure SI 2).

3 Diffuse Reflectance UV-vis (DRUV) Spectroscopy

Diffuse Reflectance UV-Vis spectroscopy (DRUV) was used to verify the correct dispersion of ZnO-NPs inside the liquid film and to confirm that ZnO-NPs did not experience chemical modification throughout the entire manipulation process. Diffuse-Reflectance UV-vis (DRUV) measurements were carried out by using a UV-2600i UV-VIS spectrophotometer 230V (Shimadzu, Milan, Italy), outfitted with an integrating sphere ISR-2600Plus operating in the wavelength range of 220 - 1400 nm to examine the optical properties of the prepared nanoparticles and CMC/ZnO-NPs films. Barium sulfate was used as a reflectance standard. Tauc plot method was used to determine the band gap energy CMC/ZnO-NPs films. Figure SI 3 shows the DRUV-Vis absorbance plot of a CMC/ZnO film. The absorption edge wavelength was observed at 375 nm, which is close to the 378 nm wavelength found from the DRUV-Vis spectrum of ZnO-NPs (Figure SI 3). From DRUV spectrum data, it is possible to

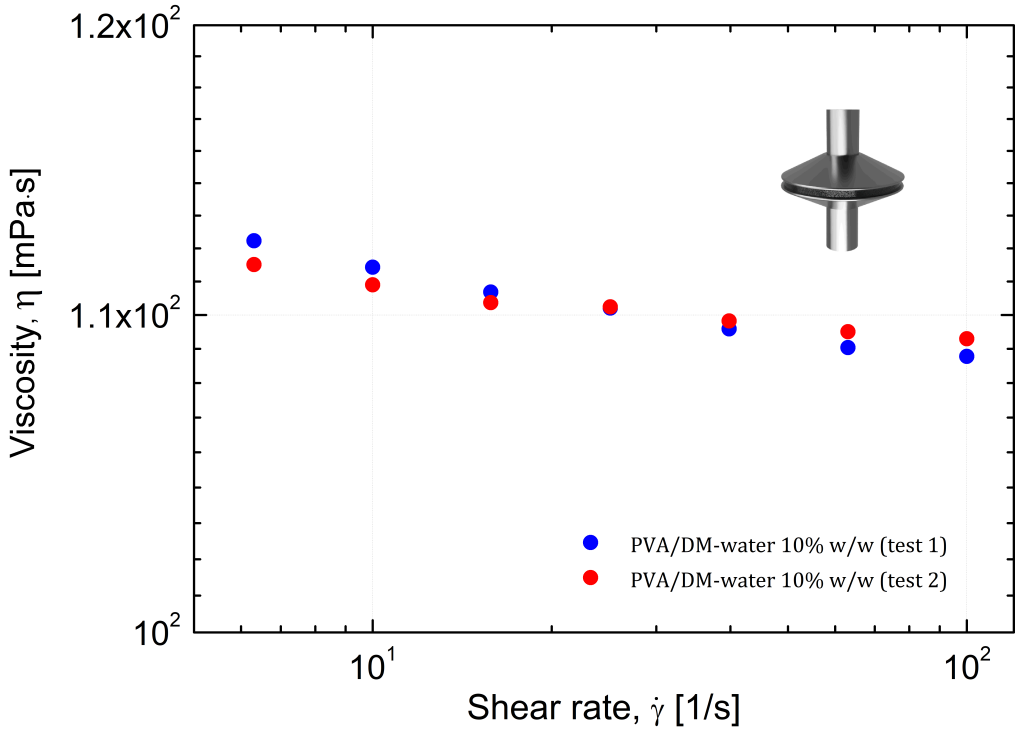

Figure SI 1: Measured viscosity (η) of the PVA/water solution 10% w/w as a function of the shear rate ($\dot{\gamma}$), repeated three times.

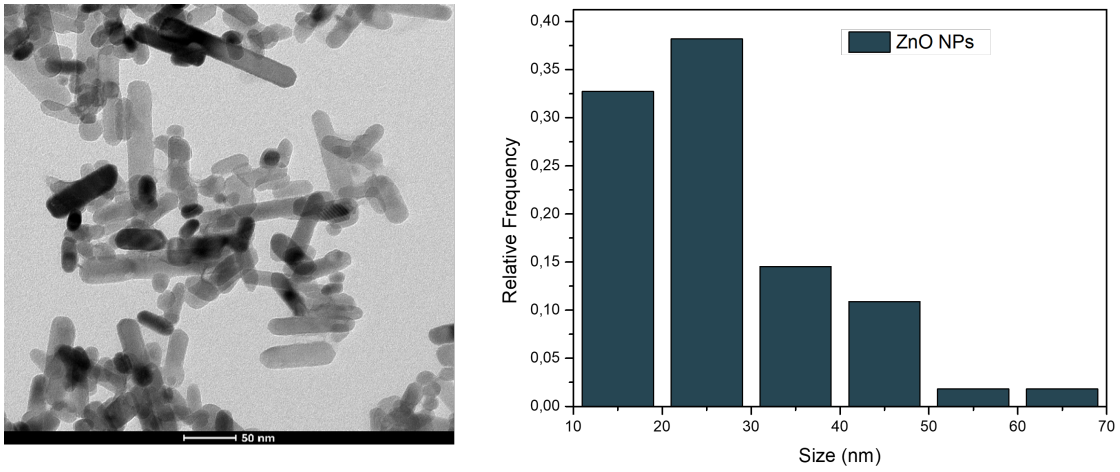

Figure SI 2: TEM image (on the left) and size distribution (on the right) of ZnO-NPs.

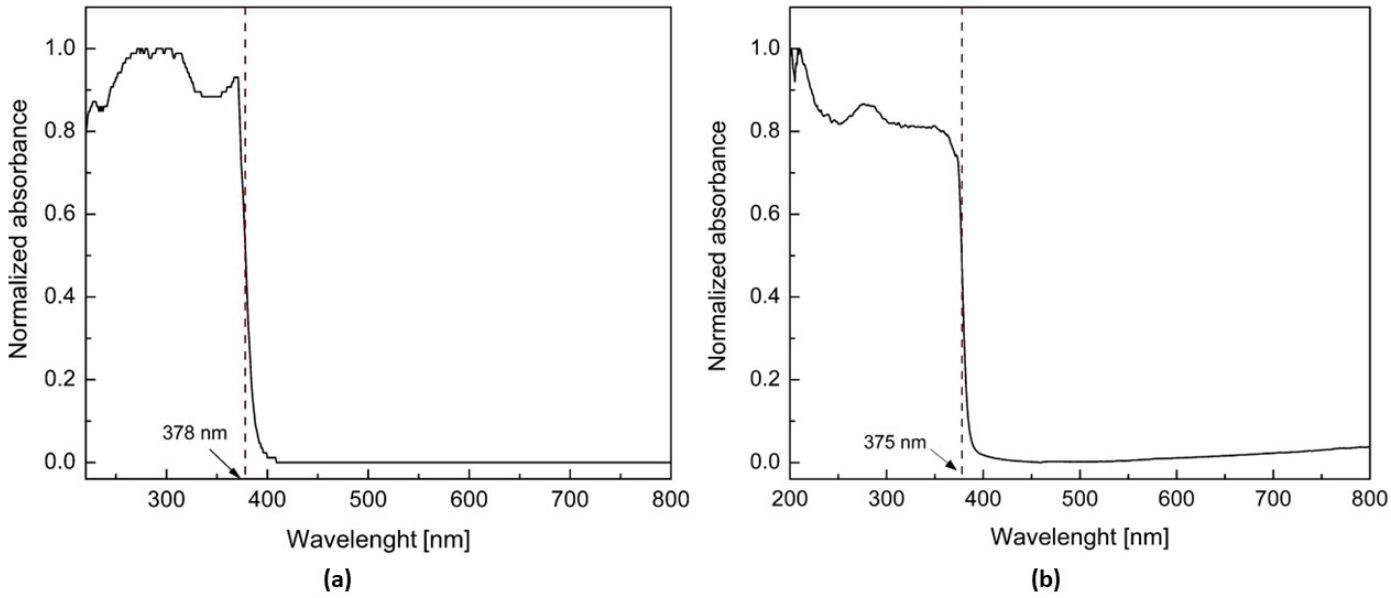

Figure SI 3: Diffuse Reflectance UV-Vis absorption spectra of ZnO NPs (a) and CMC/ZnO film (b).

estimate the energy band gap of ZnO-NPs dispersed in the polymeric film. To do so, the Tauc method was used. Figure SI 4 shows the Tauc plot obtained from the DRUV spectrum of CMC/ZnO-NPs film. The observed direct band gap energy value is 3.28 eV, consistent with the literature. This result shows that ZnO-NPs were correctly dispersed in the CMC film and that their chemical and optical properties were not modified.

4 Spatio-temporal analysis for thin free-standing film thickness

For the curves shown in Figure 4 (e-h) of the paper, angular averaging and time averaging are performed successively to draw the corresponding curves. The film thickness mapping at a certain time is firstly averaged by angle, as shown below in Figure SI 5. The "Radius" in Figure 3(a-d) of main text indicates r, which is the distance from

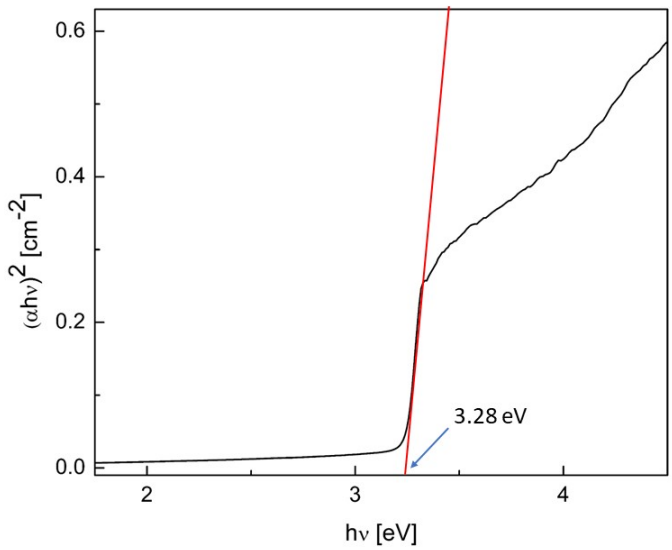

Figure SI 4: Tauc plot of CMC/ZnO film.

the geometric center of the film to the corresponding average area. To implement angular averaging between 0 and 2π, we set an additional parameter Δr, which represents the width of the ring area used for averaging. For all spatiotemporal analysis results in the manuscript, Δr is set to 2 times of actual pixel size, which is 27 μm for CCD camera and 66 μm for high-speed CMOS camera. In this case, the thickness of annular regions with the same r are averaged and projected into a new coordinate system based on time and r, as shown in Figure 3(a-d). After this, time averaging was performed to obtain the curves in Figure 4 (e-h).

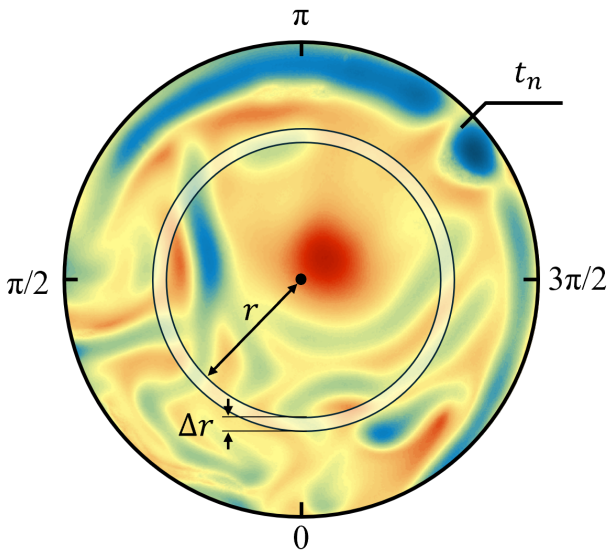

Figure SI 5: Spatio-temporal analysis of film thickness distribution at a certain time. In the figure, r represents the distance from the geometric center of the film to the corresponding average area; Δr represents the width of the annular region used for thickness averaging calculation; t_n is the selected time point.

5 Surface tension of 10% w/w PVA/water solution

The surface tension of the 10% w/w PVA/water solution is measured with the pendant drop method on a ThetaFlex OTD (Biolin Scientific). Three measurement are performed to ensure reliability of the result. The surface tension is found equal to 43.1 ± 0.2 mN/m.

6 X-Ray diffraction analysis (XRD)

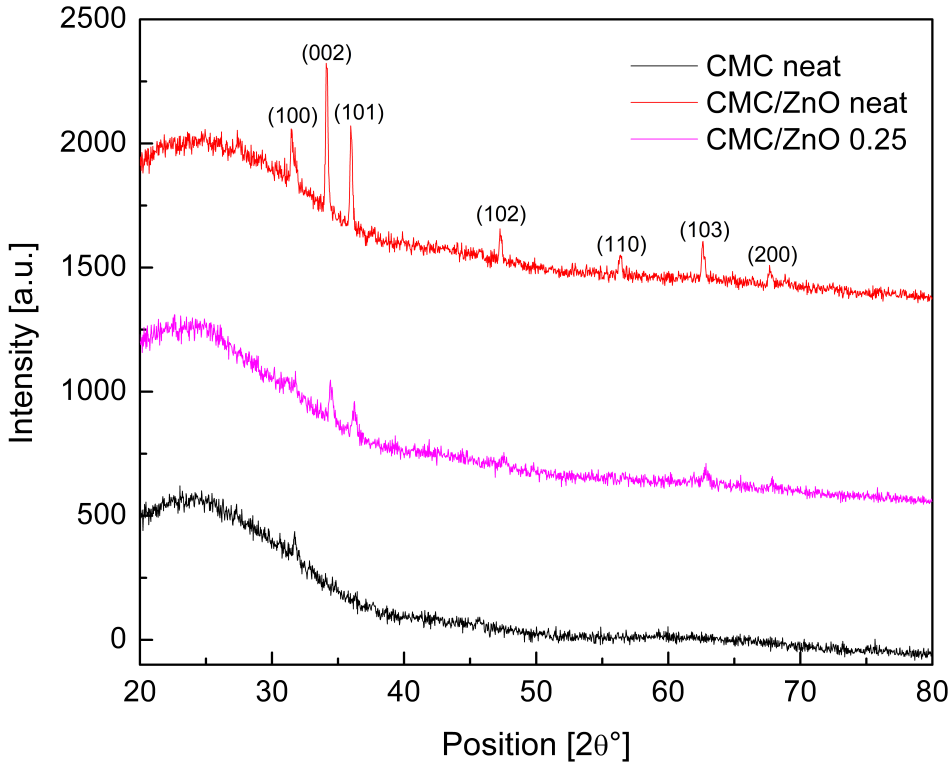

Figure SI 6: X-ray diffraction analysis results of pure CMC and CMC/ZnO-NPs films obtained using solvent evaporation and free-standing liquid film manipulation treatment.

XRD is used to obtain information about the correct inclusion and the arrangement of ZnO-NPs in the CMC film. XRD spectra in the range $5 - 80°$ were collected by using a XRD X'Pert PRO diffractometer with a step size of 0.0260° and a Cu-Kα1–2 source of λ=1.54 Å, 40 kV, and 40 mA. XRD spectra of CMC/ZnO films were obtained as well. Figure SI 6 shows the diffraction patterns obtained from a CMC film and CMC/ZnO film without any manipulation (flat-film scenario). The characteristic peaks of ZnO-NPs can be recognised from the CMC/ZnO-NPs XRD patterns and a correct inclusion of ZnO-NPs inside the film can be assessed from the data. The detected peaks are at 2θ° values of 31.5°, 34.16°, 35.96°, 47.26° and 56.39° corresponding to the (100), (002), (101), (102) and (110) lattice planes. These results were indexed as a hexagonal unit cell with wurtzite structure (JCPDS Card No. 36-1451). The peaks that arise from the presence of the ZnO-NPs are different in the case of manipulated (by periodic pumping) and non-manipulated films. In fact, the peaks of the periodic pumping manipulated film exhibit a lower intensity and their FWHM is smaller if compared to non-manipulated CMC/ZnO-NPs films. This characteristic may be related to the size of ZnO-NPs aggregates. Also, the manipulated film seems to show a smaller crystallite size, which might lead to the conclusion that the continuous transition between the two drainage regimes provides a strong force able to break apart ZnO-NPs aggregates, limiting their sorting process. However, this is only an hypothesis since FWHM is used to measure the size of crystallites in crystalline materials and not

for composite materials like the CMC/ZnO-NPs films studied in this work.

7 Evaluation of nondimensional $\Delta P(t)$ - Equation 21

Starting from the non-dimensional quantities of Equation 20 of the main article, we can write

$$\Delta P^{**}(t^*) = \frac{8\alpha^{**}(t^*)}{1+(\alpha^{**}(t^*))^2}, \tag{1}$$

that is, the non-dimensional form of Equation 16 of the main article. In this way, the non-dimensional for of the depressed cubic Equation 17 reads:

$$\alpha^{**}(t^*)^3 + c^*\alpha^{**}(t^*) + q^{**}(t^*) = 0 \tag{2}$$

where $c^{**} = 3$ and $q^*(t^*) = -6V^{**}(t^*)/\pi$. Hence, the solution is:

$$\alpha^{**}(t^*) = \sqrt[3]{\frac{3V^{**}(t^*)}{\pi} + \sqrt{\frac{9V^{**}(t^*)^2}{\pi^2}+1}} + \sqrt[3]{\frac{3V^{**}(t^*)}{\pi} - \sqrt{\frac{9V^{**}(t^*)^2}{\pi^2}+1}}, \tag{3}$$

that corresponds to the non-dimensional form of Equation 18. By substituting Equation SI 3 into Equation SI 1, Equation 21 of the main article is readily obtained.